Supporting Information

Möller-Levet et al. 10.1073/pnas.1217154110

SI Results

Temporal Patterns of Circadian Transcripts in the Control and Sleep-Restriction Condition. We used a circular self-organizing map (SOM) to identify distinctive temporal patterns within the set of prevalent circadian profiles in each condition independently. The resulting clusters display clear circadian oscillations that can be characterized primarily by their peak and trough timings (Fig. S2 *A* and *B*). Clusters 1 and 2 contain genes peaking near the onset of melatonin secretion, cluster 3 contains genes peaking near the offset of melatonin, and clusters 4 and 5 contain genes with a maximum during the biological day. The heatmaps of Fig. S2 *A* and *B* are annotated with those genes that have previously been identified as playing a role in the regulation of sleep and circadian rhythms, but we also identified many other genes with a rhythmic expression pattern. Other genes with a prominent circadian component in the control condition included: cluster 1: *CCDC85C, FBXL16*; cluster 2: *FAAH2, EPHX2, LRRN3, TCEA3, PLAG1*; cluster3: *DMRTC1*; cluster 4: *ERGIC1, TPST1, DDIT4, TMEM140*; cluster 5: *DOK4, MSL1, FOSL2,* and *AVIL*.

Genes with a circadian expression pattern that were previously associated with circadian rhythms or sleep regulation included, in the control condition: clusters 1 and 2: *NFKB2, CSNK1E, RORA, NPAS2, NR1D1, NR1D2*; cluster 3: *PER1, PER2, PER3*; clusters 4 and 5: *ARNTL* (*BMAL1*), *PRF1, PGLYRP1, GHRL, NFKB2, IL1RN, PROK2,* and *STAT3.* All rhythmic clusters showed a rising or falling trend in addition to the circadian oscillation, indicating that both time awake and circadian rhythmicity influence the expression or processing of transcripts.

Following sleep restriction, many of the genes related to sleep and circadian rhythms that were identified in the control condition as being rhythmic, remained rhythmic. Many of the genes not known to be related to sleep or circadian rhythms also remained rhythmic (e.g., *CCDC85C, FBXL16, FAAH2, EPHX2*, *LRRN3, TCEA3, PLAG1, DMRTC1, ERGIC1, TPST1, DDIT4, TMEM140, DOK4, MSL1, FOSL2, AVIL, WNT10B, SIRT2*), although some changed cluster (i.e., phase of expression) and had a reduced amplitude. Additional changes can be seen when comparing Fig. S2 *A* with *B*. Cluster 3, which previously contained all three *PER* genes in the control condition, had expanded (compared with the control condition) to include *NR1D2* and *MAT2A* (a methionine adenosyltranferase previously associated with sleep deprivation), whereas cluster 1 had reduced in size, and *PER2* had moved to cluster 4, which had an upward linear trend.

Temporal Patterns of Transcripts Responsive to Time-Awake. We identified distinctive temporal patterns within the set of prevalent time-awake–dependent genes in each condition, using a circular SOM. These time-dependent patterns (clusters) were plotted relative to the plasma melatonin rhythm, which is an established marker of the circadian pacemaker. The resulting clusters display clear upward and downward trends superimposed on a rhythmic component that differs between the clusters and sleep conditions (Fig. S2 *C* and *D*). In both sleep conditions, genes grouped into two upward-trend clusters and three downward-trend clusters. In the control condition, the most significantly up-regulated gene in cluster 1 has no known function. Other significantly up-regulated genes in cluster 1 in the control condition are *NTSR1 and PANK4.* In cluster 2, in the control condition, acute total sleep loss also resulted in significant up-regulation of the lipid transporter *ABCA1* and *PTEN.* Among the most down-regulated genes (cluster 4) was *LSG1.* The only gene known to be related to circadian rhythm or sleep that was affected by time awake in the control condition was *PROKR2*, which was up-regulated (cluster 2) with time-awake (Fig. S2*C*).

Following sleep restriction, a prominent up-regulation with time-awake was observed for *KSR1* (cluster 1) and *IMPDH1* (cluster 2). In addition, *UCP3*, *ABCA1*, *ABCG1, CEACAM3, CEACAM4*, and *CEACAM20* were up-regulated (cluster 2) in response to acute total sleep loss. A prominent down-regulation was observed for *ZNF696, LAX1*, *POP1*, and *PPM1K* (cluster 4), and *ENOX2* (cluster 5) (Fig. S2*D*).

After sleep restriction, sleep- or circadian-related genes in the two clusters with increased expression during time-awake included *IL6*, *IL1RN*, *OPN4*, *STAT3*, and *PER2.* Genes related to sleep or circadian rhythms in the three clusters with a decrease in transcript levels during acute total sleep deprivation following sleep restriction included *CRY2*, *RORA*, *CREM*, and *CAMK2D* (Fig. S2*D*).

It is noteworthy that in the control condition (Fig. S2*C*), all upward and downward clusters also showed signs of a circadian component, in particular clusters 2, 4, and 5. In the sleep-restriction condition (Fig. S2*D*), the circadian component was less prominent.

SI Methods

Study Protocol. Participants stayed indoors throughout their stay in the clinical research center. The subjects spent the majority of their waking hours in the volunteer lounge, where they could interact with the staff and other participants, watch television, listen to music, read, and play board games. Three main meals and an evening snack were provided each day and participants had free access to water and fruit (apples and pears). Napping and strenuous physical exercise were not allowed, and the participants were under continuous surveillance by staff. Participants reported consuming ≤300 mg of caffeine per day and on average 4.5 units (SD 4.4) units of alcohol per week, and were not smokers or shift workers. The participants had not traveled across more than one time zone during the 2 mo preceding the laboratory phase and had not donated blood in the preceding 6-mo period. Volunteers were not pregnant. Participants' habitual sleep timing and duration (time in bed) was assessed during a 1-wk period before the first laboratory session by the Karolinska Sleep Diary (1) and actigraphy (wrist-worn Actiwatch L or Actiwatch 4; Cambridge Neurotechnology).

Constant Routine Protocol. Upon awakening from the last sleep episode in either the sleep-restriction or control conditions, participants stayed awake for 39–41 h under constant routine conditions, which therefore represents a period of total sleep deprivation. During constant routine, participants stayed in their bed in their individual room in a semirecumbent position with light intensity <10 lx at eye level. No information related to clock time was provided. Wakefulness was monitored with a video camera and electroencephalogram and electrooculogram. Participants were not allowed to leave their bed. Participants received hourly nutritional drinks (Fortisip; Numico) instead of main meals. Blood samples were collected during a 30-h period starting 6–7 h after awakening via an indwelling cannula in the participant's forearm. This process is necessary because during the constant routine the direct masking effects of sleep may persist for several hours into the period of wakefulness and samples collected during this period could not be used to assess circadian rhythmicity nor the effects of sustained wakefulness. During the constant routine, blood samples

for assessing melatonin were collected hourly, and blood samples for total RNA extraction were taken at 3-h intervals.

Polysomnography. Electroencephalogram, electrooculogram, electromyogram, and airflow and breathing effort signals during the clinical polysomnographical test were recorded on Siesta 802 devices (Compumedics). The sampling rate and storage was 256 Hz. For the electroencephalogram signals, the low-pass filter was set at 70 Hz and the high-pass filter was set at 0.3 Hz. Electrode impedance was kept below 5 kΩ. Sleep staging was performed according to Rechtschaffen and Kales criteria (2).

Melatonin Assay and Assessment of Circadian Phase. Blood samples were centrifuged (15 min at 1,620 × *g* and 4 °C) within 20 min of collection to separate the plasma, which was then stored at −20 °C. Plasma melatonin concentration was assessed with RIA (Stockgrand). The detection limit for the melatonin assay was 3.4 pg/mL The interassay coefficients of variation were 21.9% at 8.5 ± 1.9 pg/mL (mean ± SD), 13.4% at 36.6 ± 4.9 pg/mL (mean ± SD), 13.5% at 81.0 ± 10.9 pg/mL (mean ± SD), and 11.7% at 123.5 ± 14.0 pg/mL (mean ± SD). The melatonin dim-light onset and offset were defined as the times at which the melatonin concentration crossed the value that corresponded to the baseline + 25% of the difference between the maximum and the baseline value on the rising and falling limb of the melatonin profile, respectively. The midpoint between the onset and offset was defined as the overall circadian phase and the duration of melatonin secretion was quantified as the difference between the onset and offset.

RNA Extraction, Labeling, and Microarray Hybridization and Processing. Whole peripheral blood (2.5 mL) was collected using PAXgene Blood RNA tubes (Becton Dickinson) at selected time points. Total RNA was isolated using a PAXgene Blood RNA Kit and a QiaCube robot (Qiagen). cRNA was synthesized and fluorescently labeled with Cy3-CTP from 100 ng of total RNA using the Low Input Quick Amp Labeling Kit (Agilent). Labeled cRNA (1.65 μg) was hybridized on a Whole Human Genome 4 × 44K custom oligonucleotide microarray (G2514F, AMADID 026817; Agilent) where 619 empty positions on the "off-the-shelf" array were filled in with additional probes specific for 20 clock/sleep-related genes. This custom human microarray design is deposited in the National Center for Biotechnology Institute Gene Expression Omnibus (GEO) database (www.ncbi.nlm.nih.gov/geo) and is accessible via the GEO accession no. GPL15331. Standard manufacturer's instructions for one-color gene-expression analysis were followed for labeling, hybridization and washing steps. The microarray platform design and data were submitted to the GEO archive and can be accessed using accession numbers GPL15331 and GSE39445, respectively. Extracted RNA was quantified and the $A_{260/280\ nm}$ and $A_{260/230\ nm}$ ratios were determined using a NanoDrop ND1000 spectrophotometer. RNA quality was assessed using the Bioanalyzer 2100 (Agilent Technologies). Only RNA samples with an RNA Integrity Number (RIN) >6 were subjected to microarray analysis; the majority of samples had a RIN score of >8. To minimize undesirable differences in gene expression derived from batch effects, all 20 labeled RNA samples derived from the same volunteer (10 time points taken after the control condition and 10 after sleep restriction) were processed in five 4 × 44 K Agilent Whole Human Genome slides of the same batch in a single experiment. Microarrays were hybridized at 65 °C for 17 h in an Agilent hybridization oven with rotisserie at 10 rpm. The microarrays were washed with Agilent Wash Buffer 1, prewarmed Wash Buffer 2 (37 °C), and acetonitrile, according to the manufacturer's instructions. The last washing step was performed with Agilent Stabilization and Drying Solution for 30 s. The processed microarrays were scanned using an Agilent Microarray Scanner with a resolution of 5 μm, exploiting the extended dynamic range feature. The two images derived from each slide were scanned at 10% and 100% PMT and imported into the Agilent Feature Extraction software (v10.7.1.1) for image analysis.

Microarray Statistical Analyses. ***Preprocessing.*** Individual samples were filtered based on AgilentQC metrics of reproducibility statistics, minimum detection level estimates, and feature flags [Agilent Feature Extraction Software (v10.7), *Reference Guide*, publication number G4460-90036]. Samples with a median coefficient of variation of less than 10% in spike-ins and in noncontrol replicated probes were retained and $\log_2$ values were quantile-normalized using the R Bioconductor package limma (3, 4). Noncontrol replicated probes, along with their corresponding flags, were averaged. For ANOVA analyses, probes flagged in more than five samples within a participant in more than half of the total number of participants were excluded. For time-series analyses, series with two consecutive missing time points or more than two missing time points were excluded.

ANOVA model selection. We used mixed model ANOVA as implemented in Procedure Mixed in SAS9.1 to analyze effects of Condition (Control vs. Sleep Restriction), Circadian-Time-bin (melatonin-phase-corrected sampling times), Session (reflecting the order in this cross-over design), and Genotype (because the sample was stratified for the *PER3* genotype, but as only few significant effects were observed, these will not be discussed). Note that Circadian-Time-bin (3-h-wide circadian bins) reflects the melatonin phase-aligned sampling times sorted in 45° bins to create categorical values. Because of the variance between subjects in circadian phase, this resulted in the 10 time points to cover 11 circadian bins. The general approach was to investigate whether the expression level was affected by Sleep Condition, Session, Genotype, and Circadian-Time-bin, and their simple interactions. We used Procedure Mixed because it can efficiently handle missing data in repeated measure designs and a variety of covariance structures can be selected. The direction of the significant main effects of sleep restriction on transcripts (i.e., up or down-regulated) was identified using differences in least-squares means. We subjected the time-series of each probe to three models of the covariance structure for repeated observations on the same participant.

In model 1, the repeated observations were modeled as having a constant variance irrespective of time point and different covariances depending on whether the observations were recorded within a session or between sessions, with the covariance of those between sessions being constant irrespective of sessions [i.e., if X_{ij} is the i^{th} observation for session j then $\mathrm{Var}(X_{ij}) = \sigma^2$ and $\mathrm{Cov}(X_{ij}, X_{ik}) = \Theta_1$ if $j = k$ and Θ_2 if $j \neq k$].

In model 2, the repeated observations were modeled as having different variances dependent on session, with covariances depending on whether the observations were recorded within a session or between sessions, with the covariance of those between sessions being different for different sessions [i.e., if X_{ij} is the i^{th} observation for session j then $\mathrm{Var}(X_{ij}) = \sigma_j^2$ and $\mathrm{Cov}(X_{ij}, X_{ik}) = \Theta_{jk}$].

In model 3, the repeated observations were modeled in a similar way to model 1, but imposing an autocorrelation structure on the observations for a participant within a session (i.e., observations obtained at time points closer to each other are more highly correlated than those further apart in such a way that the correlations exhibit exponential decay over the time points).

The three models were used to fit the fixed-effect model of Sleep Condition, Session, Genotype, and Circadian-Time-bin and their two-way interactions. The Akaike information criterion was used to determine the model to use.

The fixed-effect model of Sleep Condition, Session, Genotype, and Circadian-Time-bin and their two-way interactions was then reduced, maintaining the chosen covariance structure, using a step-by-step elimination process. At each stage the *F*-tests on the type 3 SS were used to determine which nonsignificant (at

5% significance level) fixed-effect or interaction was least significant. Unless this was a main effect associated with an interaction, which would remain in the model, it was removed. This process was continued until either only main-effects and interactions that were significant (at 5% level) remained or the only nonsignificant main effects remaining in the model were associated with a significant two-way interaction.

The final model was checked against the initial model, using a χ^2 test on the deviance difference, to determine whether the reduced model was significantly poorer than the original.

Identification of circadian transcripts. A curve of the form $X = a + c\ sin(t + b) + d\ t$ was fitted to each time-series using R's lm "linear model" method (5) on a linearized form of the equation $[X = a+c\ sin(b)\ cos(t) + c\ cos(b)\ sin(t) + d\ t]$ and a fixed period ~24 h (22.5, 24, and 25.5 h were used; we selected the period producing the highest R^2). In our analysis, we have added a linear trend ($d\ t$) to the sine wave as gene expression can be under both circadian and sleep-wake–dependent control. The inclusion of the linear trend improves the fit compared with standard detrending allowing for a more accurate estimation of amplitude, phase, and period. Time-series having an R^2 P value of less than 0.01, an amplitude 95% confidence interval (CI) that does not include zero, a maximum of two flagged time-points, and a coefficient of variation in the top 90th percentile were defined as circadian. Prevalent circadian genes were defined as those targeted by probes that showed a significant circadian oscillation in transcript levels in the number of participants that resulted in a false-discovery rate (FDR) of <5% in each condition.

Median profiles and alignment with the melatonin rhythm. We referenced each participant's sampling times (t) to their melatonin peak (p) by following the transformation $t_p = 24t - 24p$ (both, t and p in fractional day), where t_p is time away from the melatonin peak in hours. We then identified a time window containing sampling points for at least 50% of all participants and interpolated each participant's z-scored time-series (previously quantile-normalized on $\log_2$ values) over the resampled ($n = 60$ points) time window. Median values across all participants were calculated at each resampled point and the time window was transformed back to the range of original sampling numbers (1–10) and finally, resampled to integers. Average sampling times and melatonin across participants were then assigned to each time point.

Probe and gene numbers. The Agilent arrays used in this study typically contain one or two probes per gene. In addition, we included multiple custom probes for circadian- and sleep-related genes of interest. The primary analyses (i.e., circadian variation, expression trend, and so forth) were conducted on probes. Further analyses (i.e., gene enrichment and functional annotation) were conducted on single genes identified from significant probes. Depending on exactly when probes are converted to genes, this process can lead to some small discrepancies seen in the numbers of genes listed and those shown in the Venn diagrams of Fig. 3, for example.

Gene-Enrichment and Functional Annotation Analyses. The gene lists, detailing transcripts that were affected by sleep restriction or classified as circadian, had differential amplitudes or phases between sleep conditions, and had up and down trends with time-awake (as discussed above), were submitted to four online tools for annotation and interpretation. Agilent Probe IDs were submitted to DAVID Functional Annotation Clustering (6, 7) and MetaCore Enrichment Analysis (Thomson Reuters); the corresponding HUGO Gene Nomenclature Committee Symbol for each probe was submitted to ToppCluster (8) and WebGestalt (9). Default annotation categories/sources for DAVID were accepted and the additional protein interaction databases of BIND, MINT, and REACTOME included. For MetaCore and ToppCluster, default settings were applied. For WebGestalt, to identify the top 10 enriched processes, we used default settings with the Human genome as the reference set for the hypergeometric test. Note that this approach was also used for DAVID and MetaCore by default because this is considered as a good choice for analyses approximate to a genome-wide analysis, such as ours.

1. Akerstedt T, Hume K, Minors D, Waterhouse J (1994) The subjective meaning of good sleep, an intraindividual approach using the Karolinska Sleep Diary. *Percept Mot Skills* 79(1 Pt 1):287–296.
2. Rechtschaffen A, Kales A (1968) *A Manual of Standardized Terminology, Techniques and Scoring System for Sleep Stages of Human Subjects* (US Government Printing Office, Washington, DC).
3. Gentleman RC, et al. (2004) Bioconductor: Open software development for computational biology and bioinformatics. *Genome Biol* 5(10):R80.
4. Smyth GK (2005) *Bioinformatics and Computational Biology Solutions Using R and Bioconductor*, eds Gentleman R, Carey V, Dudoit S, Irizarry R, Huber W (Springer, New York), pp 397–420.
5. Fox J, Weisberg S (2011) *An R Companion to Applied Regression* (Sage Publications, Thousand Oaks, CA).
6. Huang da W, Sherman BT, Lempicki RA (2009) Bioinformatics enrichment tools: Paths toward the comprehensive functional analysis of large gene lists. *Nucleic Acids Res* 37(1):1–13.
7. Huang da W, Sherman BT, Lempicki RA (2009) Systematic and integrative analysis of large gene lists using DAVID bioinformatics resources. *Nat Protoc* 4(1):44–57.
8. Kaimal V, Bardes EE, Tabar SC, Jegga AG, Aronow BJ (2010) ToppCluster: A multiple gene list feature analyzer for comparative enrichment clustering and network-based dissection of biological systems. *Nucleic Acids Res* 38(Web Server issue):W96-102.
9. Duncan D, Prodduturi N, Zhang B (2010) WebGestalt2: An updated and expanded version of the Web-based Gene Set Analysis Toolkit. *BMC Bioinformatics* 11(Suppl 4):P10.

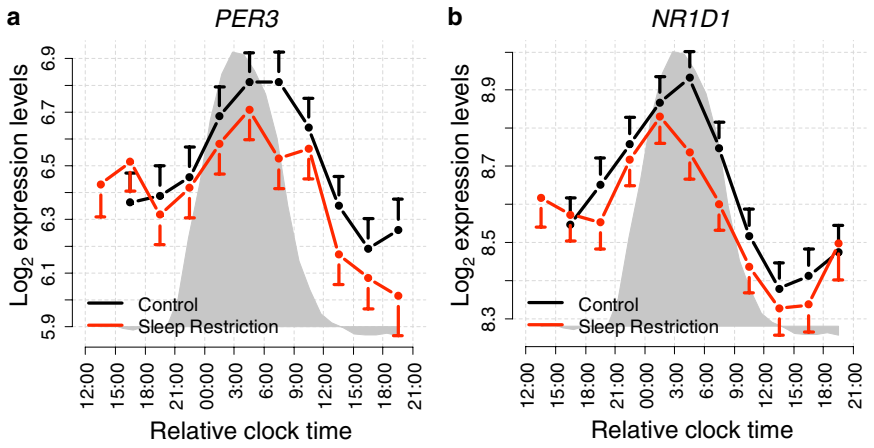

Fig. S1. (*A* and *B*) Expression profiles of genes classified as circadian in both control and sleep-restriction conditions. Mean expression profiles for each probe are shown for the control (black) and the sleep restriction conditions (red). The circadian genes *PER3* (CPID_473) and *NR1D1* (A_23_P420873) were circadian in both conditions (FDR <5%) and were not affected by sleep condition. Log_2 expression values are least-square means ± SE (Procedure Mixed, SAS). Greyed area plots represent the melatonin profile averaged for the two conditions. Note that individual data were aligned relative to the individual melatonin rhythm and sorted into discrete circadian phase bins. Because of the shift in circadian phase after sleep restriction and to individual variation, the 10 melatonin samples covered 11 circadian phase bins after sleep restriction.

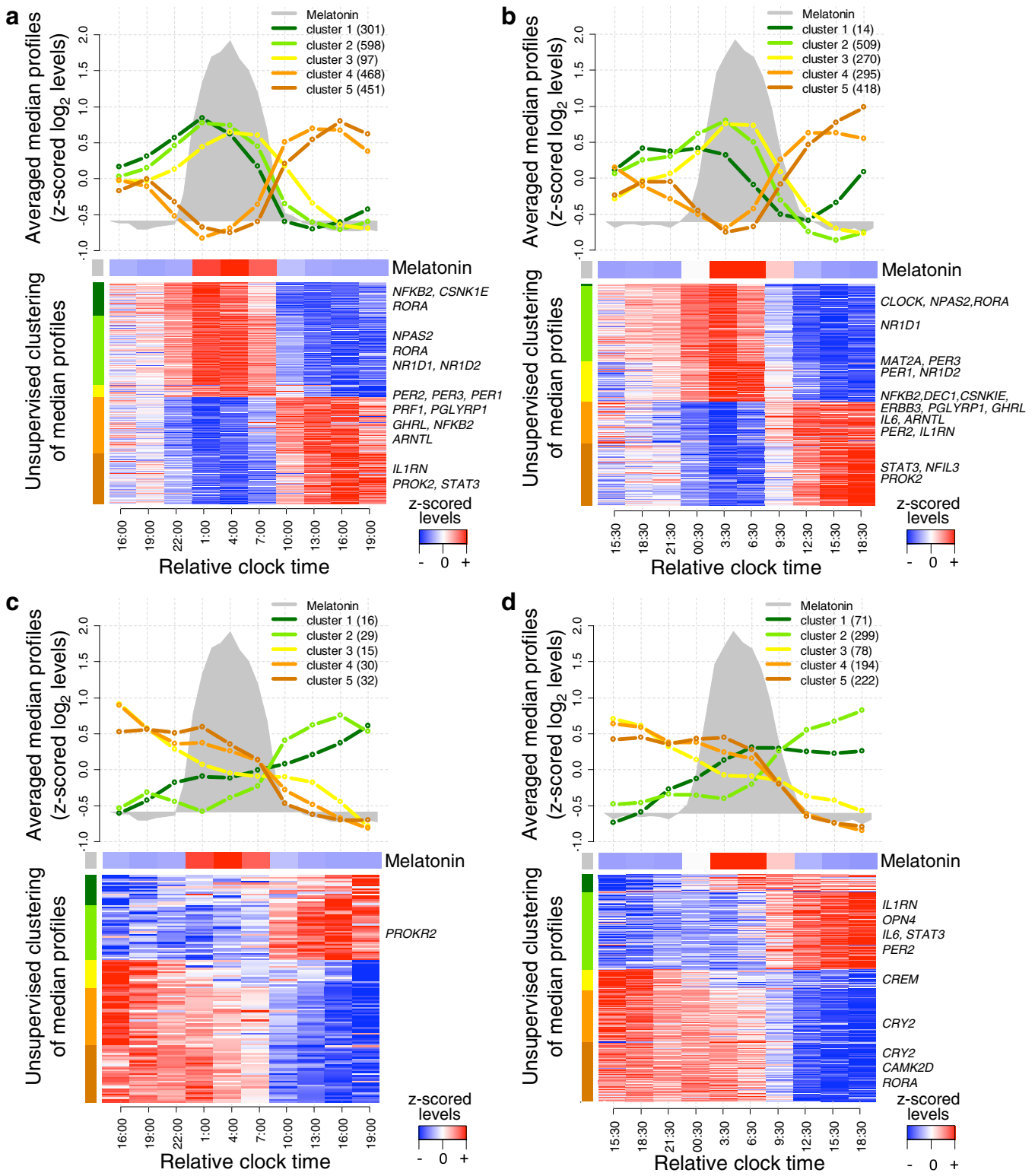

Fig. S2. Time-dependent variations in the transcriptome following Control or Sleep Restriction. Genes with a prevalent circadian variation during the constant routine/total sleep deprivation after (*A*) Control (2,103 probes that target 1,855 genes, FDR <5%) and (*B*) Sleep Restriction (1,644 probes that target 1,481 genes, FDR <5%). Genes with a prevalent time-awake–dependent variation during the constant routine/total sleep deprivation following (*C*) Control (124 probes that target 122 genes, FDR <5%) and (*D*) Sleep Restriction (890 probes that target 856 genes, FDR <5%). Heatmap rows correspond to the median of the melatonin-aligned probe values across all participants per sleep condition. Rows are clustered based on a circular SOM. Cluster means are plotted above as time-series and the number of genes per cluster is indicated in parenthesis (genes belonging to multiple clusters are counted in each cluster independently). Color codes on the left side of the heatmaps correspond to the colors of the clusters. Sampling times and melatonin profiles shown correspond to the average values across all participants per sleep condition. Genes related to circadian rhythmicity and sleep (according to Gene Ontology) are identified in the heatmaps.

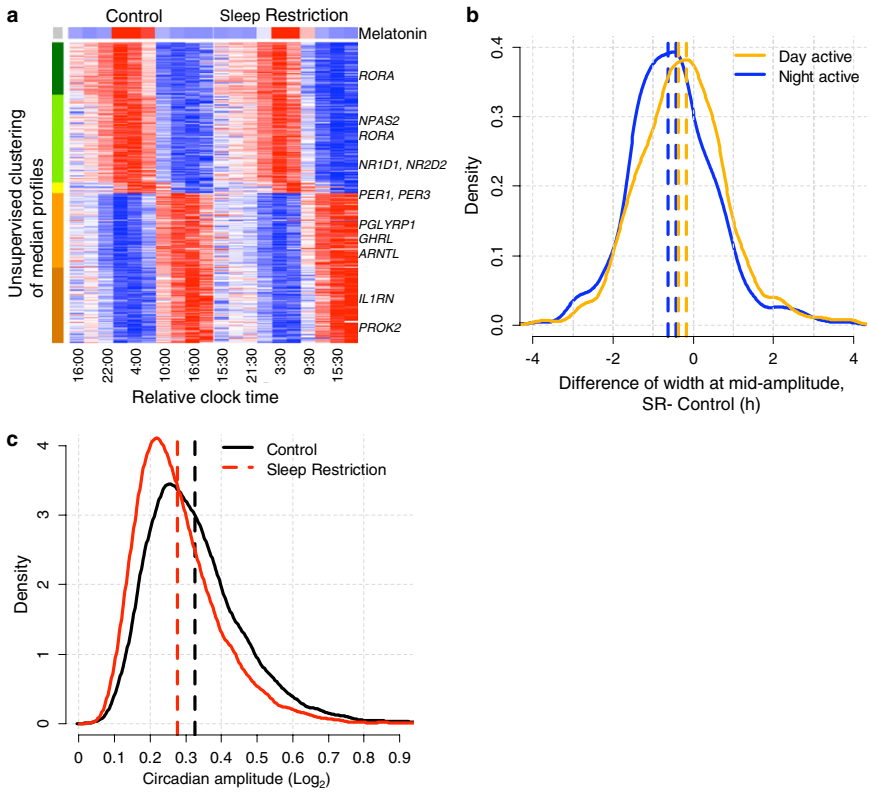

Fig. S3. Circadian variations in the transcriptome following both Control and Sleep Restriction. Genes with a prevalent circadian variation during the constant routine/total sleep deprivation after both Control and Sleep Restriction ($n = 888$ probes that target 793 genes; see Fig. 3*A*). (*A*) Heatmap rows correspond to the median of the melatonin-aligned probe values across all participants per sleep condition. Rows are clustered based on a circular SOM (based on the original complete set of prevalent circadian probes in Control). Color codes on the left side of the heatmap identify the clusters. Relative clock times and melatonin profiles shown correspond to the average values across all participants per sleep condition. Genes related to circadian rhythmicity and sleep (according to Gene Ontology) are identified in the heatmap. (*B*) Comparison of width at mid-amplitude for the night hours (trough) in the melatonin-aligned median profiles of day-active probes ($n = 442$ paired values; density of the paired differences and 95% CI are shown in orange) and comparison of width at mid-amplitude for the night hours (crest) in the night-active probes ($n = 438$ paired values; density of the paired differences and 95% CI are shown in blue). For day-active probes the estimated mean of the differences is −0.267 h [95% CI −0.374, −0.166], $P = 5.278 \times 10^{-7}$ and for the night-active probes the estimated mean of the differences is −0.530 h (95% CI −0.636, −0.425), $P < 2.2 \times 10^{-16}$. (*C*) Density plot of circadian amplitudes per participant for the prevalent circadian genes in Control or Sleep Restriction [Control $n = 11{,}014$ (black solid line) corresponding to 888 probes circadian in an average of 12.40 participants; Sleep Restriction $n = 9{,}883$ (red solid line) corresponding to 888 probes circadian in an average of 11.13 participants]. The estimated mean for the circadian amplitude is 0.326 in Control (black broken line) and 0.277 in Sleep Restriction (red broken line), difference 95% CI (−0.052, −0.046), $P < 2.2 \times 10^{-16}$.

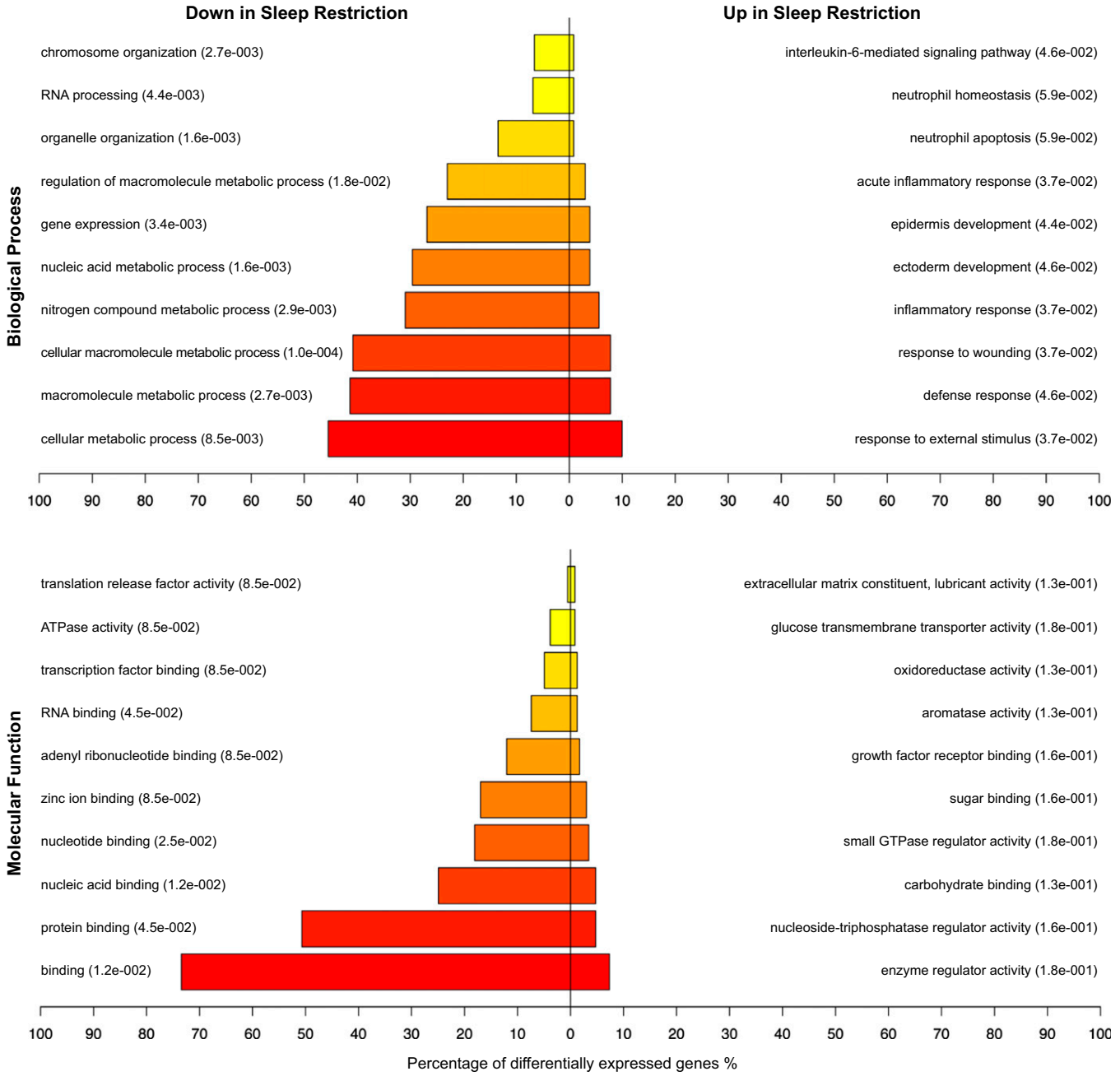

Fig. S4. Biological processes and molecular functions associated with time awake only during sleep restriction. The top 10 enriched Gene Ontology Biological Processes and Molecular Functions within the statistically significant differentially expressed gene list as identified by WebGestalt when using the human genome as a background (1). Percentages are based on the number of unique gene symbols annotated as belonging to a specific biological process/molecular function compared with the number of unique gene symbols within the entire gene list. Bar colors indicate the enrichment of a process/function, red is the most enriched (top process/function), yellow the least enriched (number 10 of the top 10). *P* values are the Benjamini and Hochberg (2) -corrected *P* values as calculated by WebGestalt (1).

1. Duncan D, Prodduturi N, Zhang B (2010) WebGestalt2: An updated and expanded version of the Web-based Gene Set Analysis Toolkit. *BMC Bioinformatics* 11(Suppl 4):P10.
2. Benjamini Y, Hochberg Y (1995) Controlling the false discovery rate: A practical and powerful approach to mulitiple testing. *J R Stat Soc, B* 57(1):289–300.

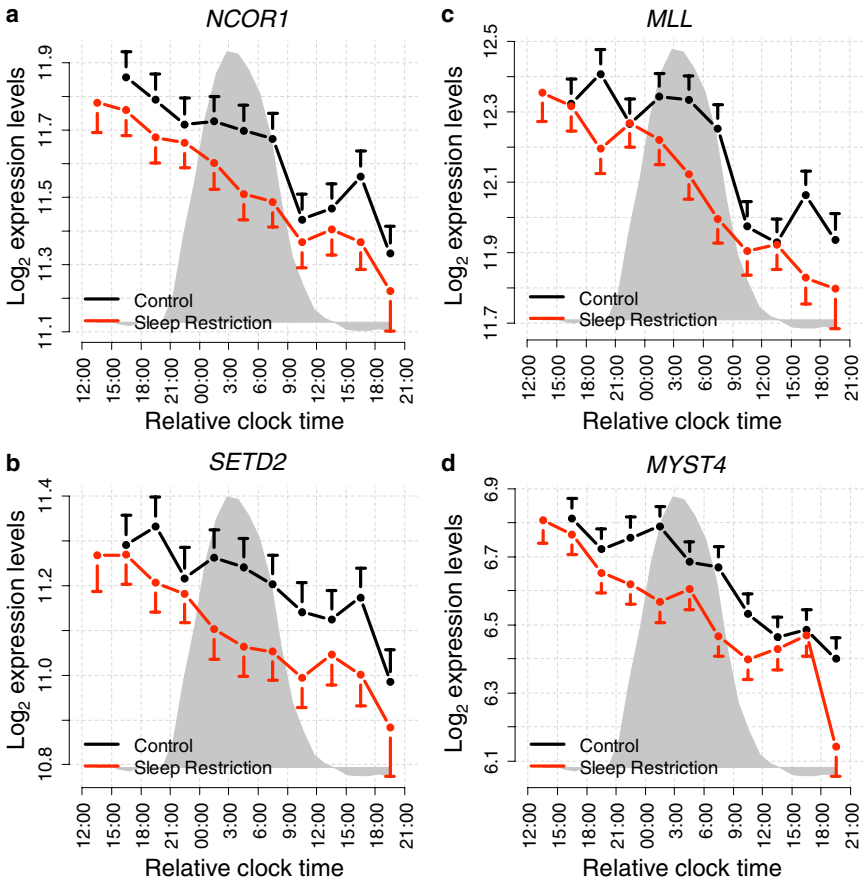

Fig. S5. (*A–D*) Expression profiles of genes that show a significant downward trend in response to sleep restriction. Mean expression profiles for each probe are shown for the control (black) and the sleep restriction conditions (red). *NCOR1* (A_24_P_204214), *MLL* (A_24_P281913), *SETD2* (A_24_P187787), and *MYST4* (A_24_P171004) were all affected by sleep condition (ANOVA-adjusted *P* values for sleep condition, $P < 0.05$ in all cases). Trend analysis showed that each probe had a downward expression profile after sleep restriction (FDR <5%). *NCOR1* had a downward expression profile in both the control and sleep restriction conditions and *MLL* appeared to have a stronger circadian component in control compared with sleep restriction. Log_2 expression values are least-squares means ± SE (Procedure Mixed, SAS). Greyed area plots represent the melatonin profile averaged for the two conditions. Note that individual data were aligned relative to the individual melatonin rhythm and sorted into discrete circadian phase bins. Because of the shift in circadian phase after sleep restriction and to individual variation, the 10 melatonin samples covered 11 circadian phase bins after sleep restriction.

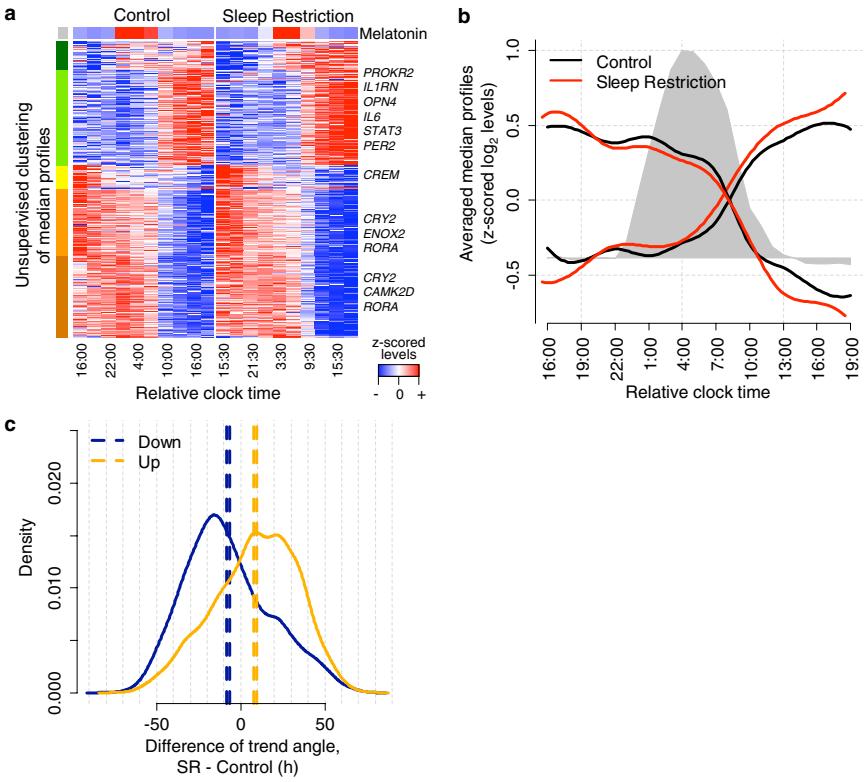

Fig. S6. Time-awake–dependent variations in the transcriptome. Genes with a prevalent time-awake variation during the constant routine/total sleep deprivation after Control and Sleep Restriction (410 probes that target 407 genes with cumulative upward trend, and 547 probes that target 516 genes with cumulative downward trend). (*A*) Heatmap rows correspond to the median of the melatonin-aligned probe values across all participants per sleep condition. Rows are ordered based on a circular SOM of the Control profiles. Color codes on the left side of the heatmap identify the clusters. Relative clock time and melatonin profile shown correspond to the average values across all participants per condition. Genes related to circadian rhythmicity and sleep (according to Gene Ontology) are identified in the heatmap. (*B*) Smoothing spline (1) of the average of melatonin-aligned median profiles (shown in *A*) of probes with an increasing trend and of probes with a decreasing trend. (*C*) Density plot of cumulative trend angle differences between Sleep Restriction and Control. A total of 2,684 paired trend angles (410 probes significant in Control and Sleep Restriction in an average of 6.54 participants) were used for the comparison of upward trends, and a total of 3,866 paired trend angles (547 probes significant in Control and Sleep Restriction in an average of 7.07 participants) were used for the comparison of downward trends. For upward trend (orange) the estimated mean of the differences is 8.6931° [95% CI (7.7490, 9.6371), indicated by orange broken lines, *t* test $P < 2.2 \times 10^{-16}$]. For downward trend (blue) the estimated mean of the differences is −7.5510° [95% CI (−8.3730, −6.7291), indicated by blue broken lines, *t* test $P < 2.2 \times 10^{-16}$].

1. Bar-Joseph Z, Gitter A, Simon I (2012) Studying and modelling dynamic biological processes using time-series gene expression data. *Nat Rev Genet* 13(8):552–564.

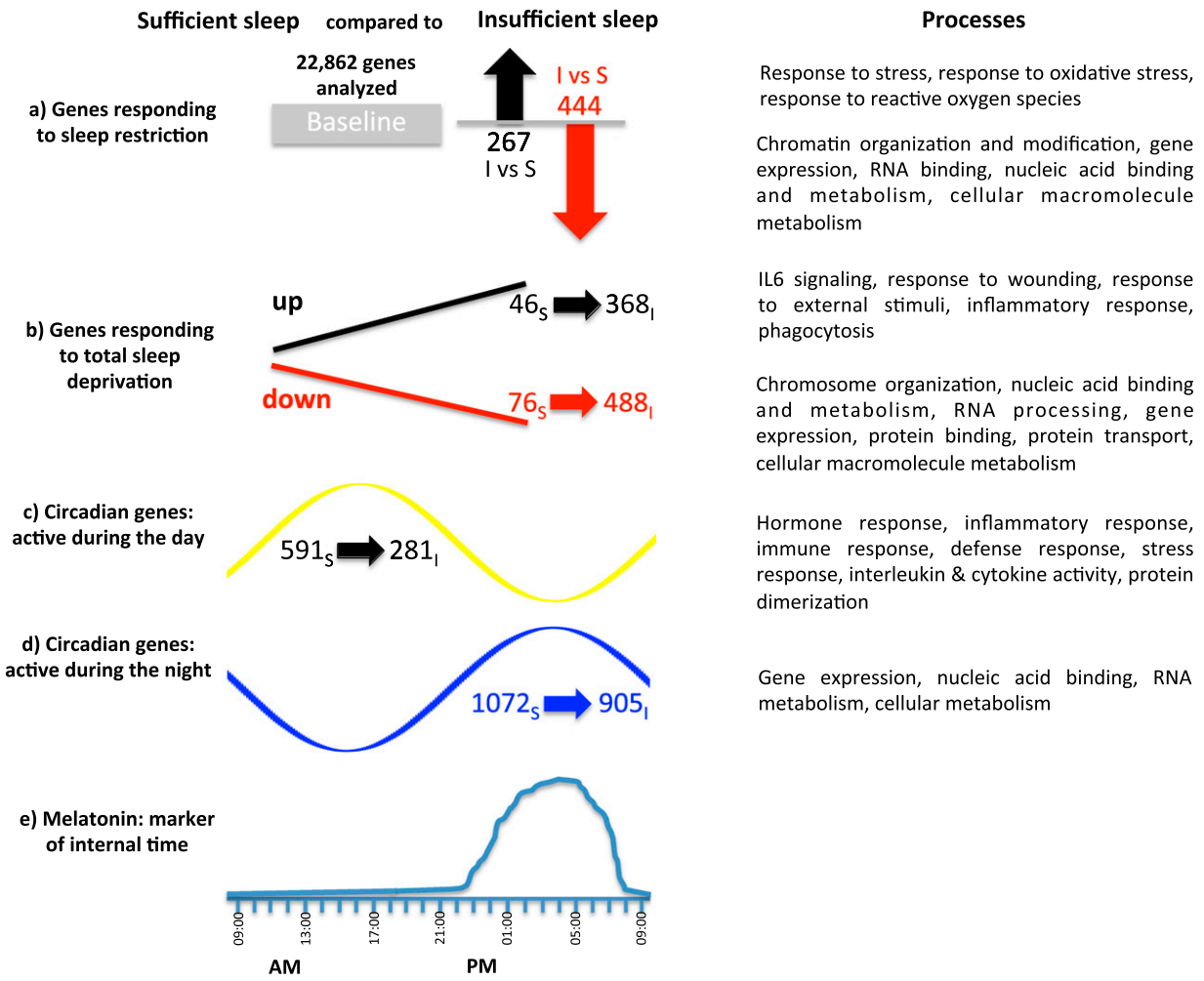

Fig. S7. Summary of the effects of insufficient and sufficient sleep on the blood transcriptome. Summary of the effects of insufficient sleep (I) compared with sufficient sleep (S) on the human blood transcriptome, and biological processes associated with these effects (numbers indicate genes affected). The panels, from top to bottom identify: (*A*) overall effects of sleep restriction; (*B*) effects of sleep restriction on the response to total sleep deprivation; effects on genes with a circadian pattern, which peak during the (*C*) day, or (*D*) night, as defined by the absence or presence of melatonin, respectively (*E*). Biological processes and functions encoded by the differentially expressed genes are indicated on the right, opposite the affected set of genes.

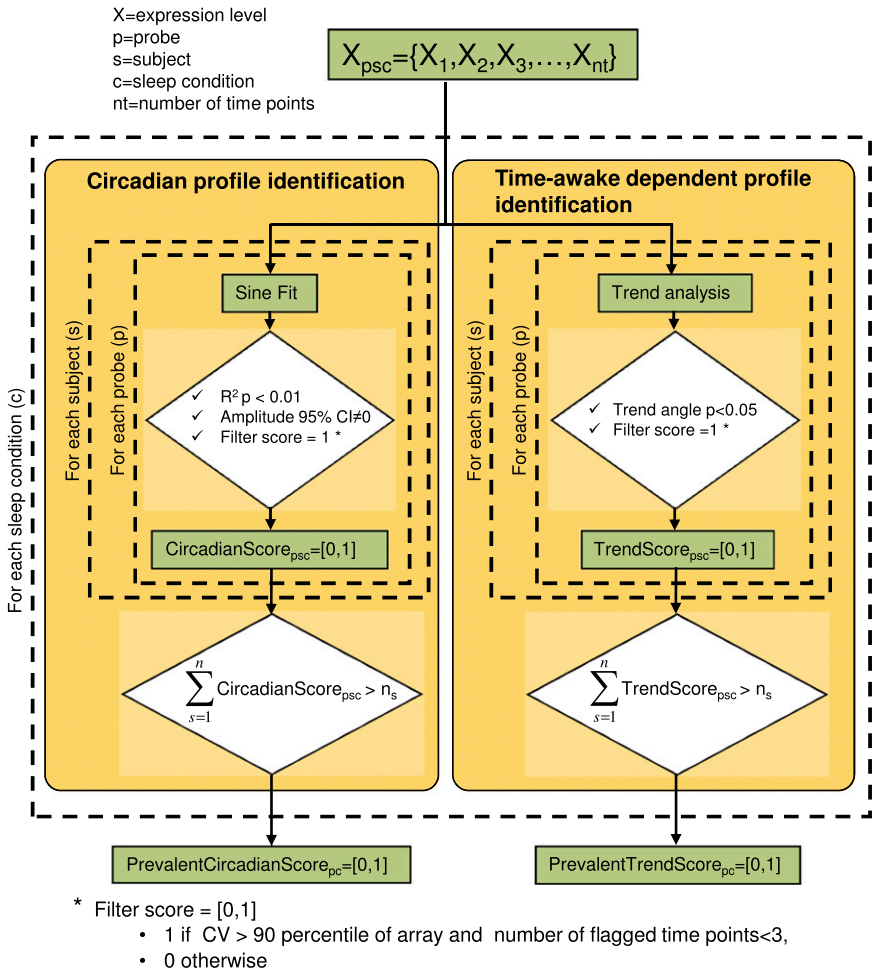

Fig. S8. Temporal pattern identification flow diagram. We defined a time-series $X_{psc} = \{X_1,X_2,X_3,.. X_{nt}\}$ as the set of *nt* time-ordered expressions levels detected by probe *p*, in participant *s*, in sleep condition *c*. The pipeline runs two parallel analyses, one for the identification of circadian profiles (*Left*) and one for the identification of time-awake–dependent profiles (*Right*). For every probe *p* in participant *s* and condition *c* (i.e., time-series X_{psc}), a circadian and a trend score are calculated. Time-series with a sine fit R^2 $P < 0.01$, a circadian amplitude 95% CI $\neq 0$, and a filter score = 1, are defined as circadian ($CircadianScorep_{sc} = 1$); time-series with a trend angle $P < 0.05$ and a filter score = 1 are defined as time-awake–dependent ($TrendScore_{psc} = 1$). The $PrevalentCircadianScore_{pc}$ and $PrevalentTrendScore_{pc}$ are then calculated per probe and sleep condition, by comparing the sum of positive scores across participants in $CircadianScore_{psc}$ and $TrendScore_{psc}$, respectively, with the threshold n_s. If the sum is at least n_s, the probe is scored positive in the corresponding prevalent score. The threshold for number of participants, n_s, is used to control the FDR (we set FDR <5%). The calculation of the FDR is based on comparing the observed distribution (number of participants in which a probe is positive) and the distribution of randomly selected probes (number of participants in which a probe is randomly assigned based on the total number of positive probes per participant).

Other Supporting Information Files

Dataset S1 (XLSX)
Dataset S2 (XLSX)